

December 10, 2009

# Proposal For the Determination of the $\rho$ -Meson Decay Width from Lattice QCD

Craig Pelissier

email: craig.pelissier@gwmail.gwu.edu

## **Advisor**

Dr. Andrei Alexandru

email: aalexan@gwu.edu

---

The increase in computing power in recent years has made it possible to study the strong interaction between hadrons using the lattice formulation of Quantum Chromodynamics (lattice QCD). The early studies are however tentative and require improvements to obtain definitive results. One objective of lattice QCD calculations is to recover experimentally known values to a high precision to confirm that QCD is the correct underlying theory of the strong interactions. Another objective is to provide information which is not accessible experimentally. For example, in the evolution of supernova it is important to understand the  $\Sigma^-$ -neutron interaction, and a lattice QCD study of this interaction would offer valuable input. In the following, we propose to study the  $\rho$  resonance appearing in the angular momentum  $l = 1$  and isospin  $I = 1$  elastic scattering channel of the two-pion system. A method for the determination of the  $\rho$ -meson decay-width and mass using lattice QCD that will improve on previous attempts is presented.

---

**The George Washington University**

# 1 Introduction

The lattice formulation of Quantum Chromodynamics (lattice QCD) has been successful in predicting hadronic quantities such as the mass spectrum, form factors, electromagnetic polarizability, etc. Recently, the lattice community has begun measuring quantities relating to scattering processes such as the phase shifts and scattering amplitudes. A method to extract these quantities using lattice QCD has actually been known for quite some time [1, 2], but the computational resources available at that time were not sufficient. Today, lattice practitioners are running fully dynamical calculations on large volumes to determine the scattering parameters for various systems. Results have been reported for meson-meson scattering, nucleon-nucleon scattering, and even simulations of many-body processes have been attempted [3]. There are several good reasons to study scattering processes using lattice QCD. One reason is simply to determine whether QCD predicts the value obtained from experiment. Another motive, perhaps more intriguing, is to determine quantities which are not experimentally known. For example, recently there was a pioneering attempt to extract the nucleon-nucleon potential [4].

In the following, we propose to extract the decay-width of the  $\rho$ -resonance from the  $I = 1$   $P$ -wave elastic  $\pi\pi$  scattering channel. The motivation for this study is to show that QCD correctly predicts the decay-width as well as to develop the tools and methodology for future investigations of this nature.  $\pi\pi$  scattering, is in a sense, the most tractable system to study. Despite this, it is still difficult to extract a reliable value for the decay-width, and there are several aspects of previous attempts that can be improved. Recent attempts to measure the decay-width were done on full QCD gauge configurations with  $N_f = 2$  flavors using clover fermions [5] and twisted mass fermions [6]. The calculations did a chiral extrapolation from unphysical kinematics with  $m_\pi/m_\rho = 0.41$ . In order to extract the decay-width, the phase shift  $\delta_1(p)$  was parameterized by the  $\rho \rightarrow \pi\pi$  coupling constant and resonance mass. The phase shift data was then fitted using this parameterization. The fits were done with at most three data points. The previous studies relied on the assumption that the coupling constant was relatively constant for pion masses in the interval 140 MeV to 390 MeV. This is supported by  $\chi$ PT [7]. The decay-width was then determined using the coupling constant in combination with the physical masses. The two results for the decay-width were

$$\Gamma = 140 \pm 27 \text{ MeV} \quad \text{and} \quad \Gamma = 50 \pm 100 \text{ MeV} \quad (1)$$

which are consistent with the experimental value of  $\Gamma = 146 \pm 1.5 \text{ MeV}$ . There are several possible avenues for improving the extraction of the decay-width. One avenue is to do the calculation at a pion mass closer to the physical value to check the predictions of chiral perturbation theory ( $\chi$ PT). It would also be desirable to generate a larger number of data points in order to achieve a more convincing fit. In light of these considerations, we will start by using a pion mass of  $m_\pi = 330 \text{ MeV}$ , which will be motivated in section 5, and generate 6-8 data points by using different box sizes. This will show definitively whether the phase shift behavior is consistent with the existence of a resonance. We will then push the mass closer the physical point in order to determine whether the coupling constant remains constant as the physical point is approached. We will calculate the  $\rho$ -meson decay-width by determining the low-lying spectrum of two-particle scattering states defined on both cubic and asymmetric spatial lattices with periodic boundary conditions. The previous studies utilized only cubic lattices, but we believe the usage of asymmetric lattices will potentially provided a more efficient way of calculating the decay-width. Having completed these calculations, we will have determined the decay-width accurately in the quenched approximation, established the appropriate lattice parameters, and implemented the required tools. Having found the appropriate lattice parameters and implemented the required tools, in the future we hope to do calculations on fully dynamical configurations as well as pursue other projects of this nature.

The paper is organized as follows. In section 2, we give a brief introduction to lattice QCD and the general technique used to calculate physical observables. In section 3, we discuss the method used to extract the  $\rho$ -meson decay-width. We then discuss in detail the extraction of the low-lying spectrum in section 4. In section 5, we explain how to estimate the appropriate lattice parameters and conclude in section 6.

## 2 Lattice QCD

In this section, we give a brief overview of the lattice formulation of QCD and the general technique used to calculate physical observables. The main objective is to familiarize the reader with the language and concepts in order to facilitate the discussions in the following sections. A complete introduction can be found in [8, 9, 10]. Currently QCD is believed to accurately model the strong interactions. It was developed in close analogy with quantum electrodynamics (QED). In particular, the concept of electric charge is identified with color and photons — the mediators of force — with gluons. Despite this formal similarity, the phenomenology of QCD is very different from that of QED. The main reason is the way the coupling constant changes with scale. Like QED, the fundamental degrees of freedom are spinorial fields but with an additional index for the *color*. The color index runs over the three colors red, blue, and green. A spinorial field in QCD is therefore represented by a  $3 \times 4$  matrix. These spinorial fields are called quark fields, and they come in six *flavors* “up”, “down”, “strange”, “charm”, “top”, and “bottom”. They are denoted by  $u(x), d(x), s(x), c(x), t(x)$  and  $b(x)$  where it is understood that when we write (say) the “up” quark as  $u(x)$ , we are referring to the  $3 \times 4$  matrix

$$u(x) = \begin{pmatrix} u_{11}(x) & u_{12}(x) & u_{13}(x) & u_{14}(x) \\ u_{21}(x) & u_{22}(x) & u_{23}(x) & u_{24}(x) \\ u_{31}(x) & u_{32}(x) & u_{33}(x) & u_{34}(x) \end{pmatrix} \quad (2)$$

where the row index corresponds to the color, the column index corresponds to the Dirac index, and  $x$  is the four-dimensional position. There is also a charge associated with each quark flavor of either  $-1/3$  or  $+2/3$ ’s of the elementary charge. Particles made up of quarks are referred to as *hadrons*, and their properties are dominated by the strong force dictated by the quark-gluon interactions. One is often interested in studying hadronic properties, but since the quarks are the fundamental degrees of freedom and not the hadrons, we can only study them indirectly. In order to extract information about hadronic systems, we will have to rely on symmetry as well as phenomenological arguments.

In the quantization of quantum field theories such as QCD, there are two equivalent approaches. In this paper, we will use both formalisms depending on which one is most apt for the discussion. It is therefore necessary to distinguish between the two methods and to make it clear how they will be referred to. The first method is to promote the fields to operators which obey certain (anti) commutation relations. We refer to this as the operatorial view. This procedure leads to the notion of creation and annihilation operators which create and destroy particles. Whenever we use the terms *operator*, *create*, or *destroy*, it is understood that we are referring to the operatorial formalism. The second approach can be introduced by considering the Euclidean correlation functions

$$C(\mathbf{x}_2, t_2; \mathbf{x}_1, t_1) = \langle 0 | T \left\{ \mathcal{O}(\mathbf{x}_2, t_2)^\dagger \mathcal{O}(\mathbf{x}_1, t_1) \right\} | 0 \rangle \quad (3)$$

Here  $\mathcal{O}(\mathbf{x}, t)$  is a time dependent operator — referred to as an *interpolating operator* — whose time-dependence is given by  $\mathcal{O}(\mathbf{x}, t) = e^{Ht} \mathcal{O}(\mathbf{x}) e^{-Ht}$  and  $|0\rangle$  represents the lowest energy state

of the system. The reason for using the Euclidean formulation is that it allows the correlation functions to be evaluated numerically. Feynman showed that the correlation function given in Eq. 3 can be written as

$$\langle 0|T \left\{ \mathcal{O}(\mathbf{x}_2, t_2)^\dagger \mathcal{O}(\mathbf{x}_1, t_1) \right\} |0\rangle = \frac{\int \mathcal{D}A \mathcal{D}\bar{\psi} \mathcal{D}\psi O(\mathbf{x}_2, t_2)^\dagger O(\mathbf{x}_1, t_1) e^{-S_{QCD}(A, \psi, \bar{\psi})}}{\int \mathcal{D}A \mathcal{D}\bar{\psi} \mathcal{D}\psi e^{-S_{QCD}(A, \psi, \bar{\psi})}} \quad (4)$$

where the RHS is called the *path integral* (PI) [11]. In this equation,  $S_{QCD}$  is the QCD action and depends on the quark fields  $\psi$  and  $\bar{\psi}$  as well as the gauge fields  $A$ , and  $T$  implies that the product is ordered such that  $t_2 > t_1$ . The quark fields are now treated as *Grassman* fields which anticommute. The integration  $\int \mathcal{D}A \mathcal{D}\bar{\psi} \mathcal{D}\psi$  is to be understood as an integration over all possible quark and gauge fields. Lastly, the operators on the LHS become Grassman fields on the RHS which is indicated by using an unscripted  $O$  and are referred to as *interpolating fields*. When we are using the PI formalism we will use the terms *interpolating fields* or *Grassman fields*.

To evaluate the correlation functions in Eq. 3, we appeal to statistical methods. In particular, we see that the PI in Eq. 3 can be viewed as the ensemble average of  $O(\mathbf{x}_2, t_2)^\dagger O(\mathbf{x}_1, t_1)$  where the probability distribution is given by

$$P(A, \psi, \bar{\psi}) = e^{-S_{QCD}(A, \psi, \bar{\psi})} / \mathcal{Z} \quad (5)$$

and the partition function is given by

$$\mathcal{Z} = \int \mathcal{D}A \mathcal{D}\bar{\psi} \mathcal{D}\psi e^{-S_{QCD}(A, \psi, \bar{\psi})} \quad (6)$$

Of course, we assume that theory is appropriately regularized so that this interpretation is well defined. The correlation function can now be thought of as the ensemble average of the product of Grassman fields  $\mathcal{O}(\mathbf{x}_2, t_2)^\dagger \mathcal{O}(\mathbf{x}_1, t_1)$ . We denote the correlation function by

$$C(\mathbf{x}_2, t_2; \mathbf{x}_1, t_1) = \left\langle \mathcal{O}(\mathbf{x}_2, t_2)^\dagger \mathcal{O}(\mathbf{x}_1, t_1) \right\rangle \quad (7)$$

The correlation functions are estimated numerically by using monte-carlo techniques. In order to apply numerical techniques, the problem is defined on a space-time lattice of finite extent. To formulate the QCD on a space-time lattice, The action must be discretized in such a way that when the lattice spacing goes to zero, i.e. the continuum limit, the original theory is recovered. After discretizing the QCD action, one finds that the PI takes the following form

$$\frac{\int \mathcal{D}U \mathcal{D}\bar{\psi} \mathcal{D}\psi O(\mathbf{x}_2, t_2)^\dagger O(\mathbf{x}_1, t_1) e^{-S_g(U) - \bar{\psi} M(U) \psi}}{\int \mathcal{D}U \mathcal{D}\bar{\psi} \mathcal{D}\psi e^{-S_g(U) - \bar{\psi} M(U) \psi}} \quad (8)$$

where  $U$  represents the gluonic degrees of freedom,  $M(U)$  is referred to as the *fermionic* matrix and  $S_g(U)$  represents the part of the action which is purely gluonic. The discussion of how to determine an estimate for the ensemble average of  $O(\mathbf{x}_2, t_2)^\dagger O(\mathbf{x}_1, t_1)$  is deferred until subsection 4.4.

At this point, we have only discussed how to determine estimates for correlation functions. We now proceed to discuss how to calculate a physical observable such as the mass of a hadronic particle. We start by examining the functional form of the correlation functions. Inserting a complete set of energy eigenkets  $|n\rangle$ , one finds

$$C(t, \mathbf{x}_2, \mathbf{x}_1) = \langle 0|O^\dagger(t_2, \mathbf{x}_2)|0\rangle \langle 0|O(t_1, \mathbf{x}_1)|0\rangle + \sum_{n=1}^{\infty} c_n^*(\mathbf{x}_2) c_n(\mathbf{x}_1) \exp(-W_n t) \quad (9)$$

where  $W_n = E_n - E_0$  with  $E_0$  representing the vacuum energy and  $E_n$  for  $n > 1$ , are the excited states,  $t = t_2 - t_1$  and  $c_n(\mathbf{x}) = \langle 0 | \mathcal{O}(\mathbf{x}) | n \rangle$ . From this equation, it is clear that for large  $t$  terms with higher energies  $W_n$  will be exponentially suppressed compared to lower energies. As a result,  $C(t, \mathbf{x}_2, \mathbf{x}_1)$  can be well approximated by a finite sum of terms  $n = 1, 2, 3, \dots$  given we make an appropriate choice of  $t$ . The time dependence of the correlation function can then be fitted with a relatively small number of parameters and the low-lying energies  $W_n$  can be determined. While these energies belong to the QCD spectrum, we have not established a way to identify the energies  $W_n$  with the energy of a particular physical system. For instance, if we are interested in measuring the mass of the pion we would need to identify an energy  $W_n$  as the energy of a single pion having zero-momentum. Moreover, from a practical stand-point it would have to appear as one of the low-lying energies in the correlator we compute. To do this, we rely on symmetry arguments. In particular, what we can do is create a *filter* which selects the energies in the spectral decomposition of the correlation function defined in Eq. 9 that correspond to physical systems having certain symmetries. For example, by examining how the correlation function behaves under parity we can create a filter which leaves only the energies which correspond to states with a definite parity. As a concrete example, we consider the physical system of a pion at rest with a charge of  $+1$ , i.e.  $\pi^+$ .  $\pi^+$  is comprised of an “up” and “anti-down” quark. It has spin zero and negative parity. We will then create a filter which selects the states comprised of an “up” and “anti-down” quark with these quantum numbers. We will show in subsection 4.1 that such a filter can be created by imposing these conditions on the operators appearing in the correlation function. The lowest energy which contributes to the corresponding correlation function will then correspond to the pseudoscalar hadron with the smallest mass which is comprised of an “up” and a “anti-down” quark. Phenomenologically we know this is the pion, and therefore we associate the lowest energy determined from the fit with the mass of the pion.

### 3 Extraction of the Decay-Width

As previously discussed, the quantity that is most readily accessible using lattice QCD is the low-lying energy spectrum. In light of this, it is necessary to find formulae relating the two-particle spectrum to the scattering parameters. Such formulae were proposed by M. Lüscher for the two-particle scattering states of massive scalar field theories defined on a 3D-torus. Specifically, they relate the two-particle spectrum to scattering parameters such as the phase shifts, amplitudes and scattering lengths. However, there are several practical difficulties that arise. In this section, we will present the formulae relevant for calculating the  $\rho$ -meson decay-width. In doing so the difficulties of the method will become apparent. There will be no attempt to justify the formulae presented. The justifications are non-trivial and the interested reader should refer to the original papers [1, 2].

#### 3.1 Calculation of the scattering parameters

In this study, we are interested in the two-pion scattering states defined on a 3D-torus, i.e. a box with linear extent  $L$  and periodic boundary conditions. This system has a resonance in the  $I = 1$   $P$ -wave channel which is attributed to the creation of an unstable  $\rho$ -meson. One can use Lüscher’s formulae to study the  $\rho$ -resonance by calculating the scattering phase shifts in this channel. We first consider the case where the pions have zero total-momentum. The energy of the two-pion states is defined thru the relation

$$W = 2\sqrt{m_\pi^2 + p^2} \quad (10)$$

In the non-interacting case  $p$  coincides with the relative momentum of the two-pions. Lüscher's formula then reads

$$\delta_1(p) = \tan^{-1} \left\{ \frac{\pi^{3/2} q}{Z_{00}(1, q^2)} \right\} \bmod \pi \quad (11)$$

where  $p$  is defined through Eq. 10,  $L$  is the length of the period, taken to be the same in all direction, and  $Z_{lm}(s, q^2)$  is the generalized zeta function defined by

$$Z_{lm}(s, q^2) = \sum_{\mathbf{n} \in \mathbb{Z}^3} \frac{n^l Y_{lm}(\Omega_{\mathbf{n}})}{(\mathbf{n}^2 - q^2)^s} \quad q = \frac{pL}{2\pi} \quad (12)$$

From this formula it is evident that if the energy spectrum can be determined the phase shifts can be extracted. This equation makes three main assumptions: (1) the box size is greater than the range of the interaction and large enough so that finite volume effects are negligible (2) the angular momenta  $l \geq 3$  vanish and (3) the energy is in the elastic scattering region  $2m_\pi \leq W \leq 4m_\pi$ . The first and third reasons are somewhat intuitively obvious. The second assumption is less obvious. It arises from the fact that on a 3D-torus the symmetry group of the Hamiltonian is reduced from the full rotation group to the subset of cubic rotations. The details are deferred until subsection 4.1. To get a feeling for this formula, we consider the non-interacting case. In this case  $p$  is the magnitude of the relative momentum. As a result of the periodic boundary conditions the momenta are quantized and take the values

$$\mathbf{p}_{\mathbf{n}} = \frac{2\pi}{L} \mathbf{n} \quad \mathbf{n} \in \mathbb{Z}^3 \quad (13)$$

In this case,  $q^2$  takes on only integer values and  $Z_{00}(1, q^2)$  diverges for all momenta. The phase shift is then given by

$$\delta_1(p) = \frac{\pi}{2} \quad (14)$$

As one would expect the phase shift remains constant.

About a decade ago, Rummukainen and Gottlieb extended Lüscher's formulae to systems with a non-zero total momenta [12]. The basic idea is to measure the energy in the lab frame where the two-particles have non-zero total-momentum and relate it to the CM energy where the finite volume formulae derived by Lüscher are valid. To understand the advantages of this method, we consider the case of two non-interacting particles. The energies in the CM and lab frame are given by

$$W_L = \sqrt{m^2 + \mathbf{p}_1^2} + \sqrt{m^2 + \mathbf{p}_2^2} \quad \text{and} \quad W_{CM} = 2\sqrt{m^2 + \mathbf{p}^2} \quad (15)$$

where we have taken the masses to be degenerate. Letting  $\mathbf{P}$  denote the total-momentum, the two invariant energies are related by

$$W_{CM}^2 = W_L^2 - \mathbf{P}^2 \quad (16)$$

where  $\mathbf{P} = \frac{2\pi}{L} \mathbf{d}$  and  $\mathbf{d} \in \mathbb{Z}^3$ . In Fig. 1, the energies of the non-interacting particles are plotted as a function of the box size.

The dashed lines are the energies in the CM when the lab frame and CM frame coincide, and the solid lines are the energies in the CM when the lab is moving with a momentum  $2\pi/L\vec{\mathbf{e}}_z$  with respect to the CM frame. For example, the first dashed line represents the ground state energy as a function of the box size. The second dashed line corresponds to the first excited state and so on.

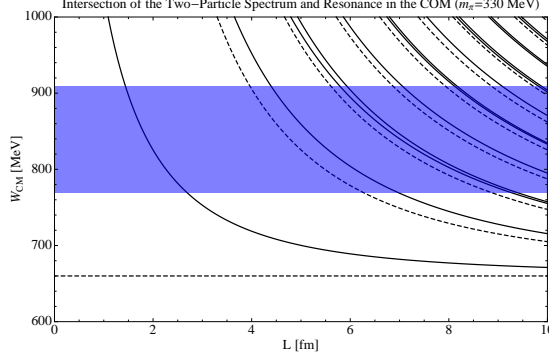


Figure 1: In this figure, the non-interacting two-particle spectrum is plotted for  $m_\pi = 330$  MeV. The dashed lines correspond to the CM energies obtained when the lab frame and CM coincide. The solid lines represent the spectrum in the CM when the lab frame and CM are moving relative to each other with a momentum  $\mathbf{P} = \frac{2\pi}{L}\mathbf{e}_z$ . The blue bands represent the energy regime where the  $\rho$  resonance occurs. In order to determine in what range  $\rho$  will decay, we estimate  $m_\rho$  by looking at previously determined values of  $(m_\pi, m_\rho)$  in the literature and take the decay-width to be the same as the physical one.

Likewise for the solid lines. The blue bands represent the energy regime for the  $\rho$  resonance. This regime is not known *a priori* for non-physical pion masses. In order to determine in what energy range  $\rho$  will decay for unphysical pion masses, we estimate  $m_\rho$  by looking at previously determined values of  $(m_\pi, m_\rho)$  in the literature [5, 13]. The decay-width is taken to be the same as the physical one. A few comments on relevance of these graphs are in order. First, in order to extract the  $\rho$  decay-width, we need the values of the energy spectrum which fall in the energy band where  $\rho$  decays. This energy regime is represented in Fig. 1 by a blue band. It is clear that the dimensions of the box size cannot be arbitrarily chosen if one hopes to have the ground or first excited state fall in the energy regime where  $\rho$  decays. The second thing to notice is that when the lab frame and CM coincide, the lowest state that falls in the decay-band is the first excited state, while in the case of a non-zero total momentum it is the ground state. However, since the  $\rho$  decays in the angular momentum  $l = 1$  channel the state with  $\mathbf{p} = 0$  will not appear in the spectrum. Lastly, the size of the lattice required is substantially less in the moving frame. The relation between the phase shifts and the spectrum in the lab frame is dependent on the relative velocity between the CM and lab frame as well as the particular channel being investigated. In this case, we have chosen  $\mathbf{P}$  to be along the  $z$ -axis. Therefore, when we boost into the CM frame the length of the box in the  $z$ -direction becomes elongated, and as a result the rotational symmetry is reduced from the cubic rotations to the tetragonal rotations. The tetragonal rotations consist of the set of cubic rotations which leave the  $z$ -coordinate either reflected or invariant. For the case of  $P$ -wave scattering with total-momentum  $\mathbf{P} = 2\pi/L\mathbf{d}$  in the  $z$ -direction, the relevant formulae are

$$\tan \delta_1^{A_2^-}(p) = \frac{1}{q\gamma\pi^{3/2}} \left\{ Z_{00}^{\mathbf{d}}(1; q^2) + \frac{2}{\sqrt{5}} q^{-2} Z_{20}^{\mathbf{d}}(1; q^2) \right\} \quad (17)$$

$$\tan \delta_1^{E^-}(p) = \frac{1}{q\gamma\pi^{3/2}} \left\{ Z_{00}^{\mathbf{d}}(1; q^2) - \frac{1}{\sqrt{5}} q^{-2} Z_{20}^{\mathbf{d}}(1; q^2) \right\} \quad (18)$$

where  $A_2^-$  and  $E^-$  denote irreducible representations of the tetragonal group and  $\mathbf{d}$  indicates that the sum in Eq 12 is now to be taken over the set

$$\Gamma = \left\{ \mathbf{r} \in \mathbb{R}^3 \mid \mathbf{r} = \tilde{\gamma}^{-1}(\mathbf{n} + \frac{1}{2}\mathbf{d}), \mathbf{n} \in \mathbb{Z}^3 \right\} \quad (19)$$

where

$$\tilde{\gamma}\mathbf{n} = \gamma\mathbf{n}_\perp + \mathbf{n}_\parallel \quad \text{and} \quad \tilde{\gamma}^{-1}\mathbf{n} = \gamma^{-1}\mathbf{n}_\perp + \mathbf{n}_\parallel \quad (20)$$

At this point, it is unclear how the irreducible representations of the tetragonal group are relevant for determining the  $P$ -wave scattering phase shifts. This will be clarified in subsection 4.1.

The advantages of looking at the two-particle spectrum of states with non zero-total momentum is that the boxes required are smaller. An alternative method is to consider the two-particle scattering states with zero total-momentum defined on elongated boxes, i.e asymmetrical boxes with  $L_x = L_y \neq L_z$ . In this case, the energy of the first excited state will correspond to the two-particle state with relative momentum  $2\pi/L_z$  in the  $z$ -direction. This follows from the fact that  $2\pi/L_z < 2\pi/L_x = 2\pi/L_y$ . Therefore by increasing the linear extent of the box in the  $z$ -direction and keeping the other two directions fixed, one can vary the first excited state over the energy regime where the  $\rho$  decays. The additional computational resources associated with increasing the box size in *one* direction will be slightly larger. However, in general more statistics are required to extract the energy of non zero total-momentum states and as a result the usage of asymmetric boxes may potentially be more efficient. The relevant formulae for boxes elongated in the  $z$ -direction are

$$\tan \delta_1^{A_2^-}(p) = \frac{1}{q\pi^{3/2}} \left\{ Z_{00}(1; q^2) + \frac{2}{\sqrt{5}}q^{-2}Z_{20}(1; q^2) \right\} \quad (21)$$

$$\tan \delta_1^{E^-}(p) = \frac{1}{q\pi^{3/2}} \left\{ Z_{00}(1; q^2) - \frac{1}{\sqrt{5}}q^{-2}Z_{20}(1; q^2) \right\} \quad (22)$$

where the generalized zeta function  $Z_{lm}(1; q^2)$  is now summed over the set

$$\Gamma = \left\{ \mathbf{r} \in \mathbb{R}^3 \mid \mathbf{r} = \left\{ n_x, n_y, \frac{L}{L_z}n_z \right\} \text{ where } \mathbf{n} \in \mathbb{Z}^3 \text{ and } L = L_x = L_y \right\} \quad (23)$$

### 3.2 Chiral extrapolation

For practical reasons, it is advantageous to do lattice calculations with pion masses heavier than the physical pion mass and extrapolate to the physical point using an effective field theory. Phenomenologically, the scattering phase shift  $\delta_1(p)$  is well described by the effective range formula

$$\frac{p^3}{W} \cot \delta_1(p) = \frac{24\pi}{g_{\rho\pi\pi}^2} (p_{phys}^2 - p^2) \quad (24)$$

where  $p$  is defined through Eq. 15,  $p_{phys} = 1/2\sqrt{M_\rho^2 - 4m_\pi^2}$ , and  $g_{\rho\pi\pi}$  is the coupling constant defined through the effective Lagrange

$$\mathcal{L}_{\text{eff}} = g_{\rho\pi\pi} \sum_{abc} \epsilon_{abc} (p_1 - p_2)_\mu \rho_\mu^a(p) \pi^b(p_1) \pi^c(p_2) \quad (25)$$

The decay-width  $\Gamma$  in this model is given by

$$\Gamma = \frac{g_{\rho\pi\pi}^2 p_{phys}^3}{6\pi m_\rho^2} \quad (26)$$



The coupling constant will in general be a function of the pion mass. There has been recent studies both lattice and theoretical [7] that have indicated that the coupling constant becomes nearly independent of the pion mass as it approaches the physical point. If the simulation is done for multiple pion masses approaching the physical point and the coupling constant does not vary appreciably, one can assume that the coupling constant obtained is in fact the physical one. With this assumption, the decay-width can be determined from Eq. 26 in combination with the physical  $\rho$  mass and momentum. Namely,

$$m_\pi = 140 \text{ MeV}, \quad m_\rho = 770 \text{ MeV}, \quad \text{and} \quad p^2 = m_\rho^2/4 - m_\pi^2 \quad (27)$$

## 4 Extraction of the Low-Lying Energies

As seen from section 2, in order to apply the finite volume formulae to extract scattering parameters, one must extract the first few low-lying energies of the scattered particles. In this study, we are interested in extracting the width of the  $\rho$  resonance. Therefore, we are interested in the low-lying energy spectrum of the two-pion states with isospin  $I = 1$  and angular momentum  $l = 1$ . In the following section, we discuss in detail the procedure for extracting the low-lying energies.

### 4.1 Projection onto the symmetry groups

At this point, it is evident that a firm understanding of symmetries is required to calculate physical observables using lattice QCD. In this study, we are interested in creating interpolating fields with fixed total-momentum and with a certain angular momentum, parity and isospin. While on the lattice there are fewer symmetries, it is still possible to implement exactly translational invariance, parity and isospin. However, as we will see, it will not be possible to classify a state with a single angular momentum. This was alluded to in section 3.1, when the formulae were labeled with the irreducible representations of the tetragonal group and not by an angular momentum  $l$ . As discussed in subsection 2, this procedure allows us to isolate the part of the QCD spectrum with these quantum numbers which enables one to identify energies with a particular physical system. In this section, we give an overview of the relevant symmetries and develop the tools required to implement them.

We start by discussing how to isolate the part of spectrum corresponding to certain quantum numbers where the quantum numbers (labels) refer to a particular irreducible representation of a symmetry group. In order to do this, we must create a filter which selects only the states having certain quantum numbers. Such a filter can be created by considering the correlation of operators which are projected onto the irreducible representation of the symmetry group  $G$  of interest. The projection operator for discrete groups is given by

$$P_\mu = \frac{n_\mu}{g} \sum_{g \in G} \chi^\mu(R) O_R \quad (28)$$

where  $\mu$  (i.e. the quantum number) labels the irreducible representation,  $n_\mu$  is the dimension of the representation,  $g$  is the number of elements in the group, and  $\chi^\mu(R)$  and  $O_R$  are the character and operator associated with the element  $R$  [14]. The projected operator  $\mathcal{O}_P(\mathbf{x}, t)$  is then given by

$$\mathcal{O}_P(\mathbf{x}, t) = \frac{n_\mu}{g} \sum_{R \in G} \chi^\mu(R) \mathcal{O}_R \mathcal{O}(\mathbf{x}, t) \quad (29)$$

$$= \frac{n_\mu}{g} \sum_{R \in G} \chi^\mu(R) U^\dagger(R) \mathcal{O}(\mathbf{x}, t) U(R) \quad (30)$$

$$= \frac{n_\mu}{g} \sum_{R \in G} \chi^\mu(R) \mathcal{O}(R^{-1} \mathbf{x}, t) \quad (31)$$

The correlation function of the projected operators reads

$$C(t, \mathbf{x}_2, \mathbf{x}_1) = \langle 0 | \mathcal{O}_P^\dagger(\mathbf{x}_2, t_2) \mathcal{O}_P(\mathbf{x}_1, t_1) | 0 \rangle \quad (32)$$

$$= \sum_n \langle 0 | \mathcal{O}_P^\dagger(\mathbf{x}_2, t_2) | n \rangle \langle n | \mathcal{O}_P(\mathbf{x}_1, t_1) | 0 \rangle \quad (33)$$

$$= \sum_n \langle 0 | \frac{n_\mu}{g} \sum_{R \in G} \chi^\mu(R) U^\dagger(R) \mathcal{O}^\dagger(\mathbf{x}_2, t_2) U(R) | n \rangle \times \langle n | \frac{n_\mu}{g} \sum_{R \in G} \chi^\mu(R) U^\dagger(R) \mathcal{O}(\mathbf{x}_1, t_1) U(R) | 0 \rangle \quad (34)$$

Given that the vacuum is invariant under the action of  $G$ , one finds

$$C(t, \mathbf{x}_2, \mathbf{x}_1) = \langle 0 | \mathcal{O}^\dagger(\mathbf{x}_2, t_2) | P_\mu n \rangle \langle P_\mu n | \mathcal{O}(\mathbf{x}_1, t_1) | 0 \rangle \quad (35)$$

This is precisely the filter we were looking for. The components of the states which do not belong to the  $\mu^{th}$  irreducible representation are projected out. If the state has no overlap, then  $|P_\mu n\rangle = 0$  and the energy associated with this state will not appear in the spectral decomposition of the correlation function. Lastly, we note that since the prescription for converting between the operatorial view and PI view is to replace the operators appearing in Eq. 35 by interpolating fields this result holds equivalently in the PI formalism.

We proceed to determine which symmetries are realized and which symmetries the Hamiltonian is invariant under in order to classify the eigenfunctions. The formulae relating the scattering phase shifts to the spectrum were defined on a box with periodic boundary conditions, and as a result it is necessary to consider the set of two-particle periodic states  $\psi(\mathbf{x}_1, \mathbf{x}_2)$ . There are two cases to consider: (1) the case where the periods are equal, i.e  $L_x = L_y = L_z$  and (2) the case in which  $L_x = L_y \neq L_z$ . We begin by discussing rotational symmetry in case 1. In particular, we find that the full rotation group is no longer realized, that is to say, the action of the group does not preserve the condition of periodicity. We can determine which rotations preserve the periodicity as follows: Let  $P$  denote the vector space of two-particle periodic states which have the defining condition

$$\psi(\mathbf{x}_1, \mathbf{x}_2) = \psi(\mathbf{x}_1 + \mathbf{n}L, \mathbf{x}_2 + \mathbf{m}L) \quad \mathbf{n}, \mathbf{m} \in \mathbb{Z}^3 \quad (36)$$

The subset of the full rotation group which maps *any* element of  $P$  to a subset of  $P$  must obey the additional condition

$$D(R)\mathbf{n} = \mathbf{n}' \quad D(R)\mathbf{m} = \mathbf{m}' \quad \mathbf{n}', \mathbf{m}' \in \mathbb{Z}^3 \quad (37)$$

where  $D(R)$  is a representation of the group on  $P$ . An arbitrary rotation will not satisfy this condition. The subset of the full rotation group  $SO(3)$  which satisfies this condition is the *octahedral* group. The octahedral group is often referred to as the *cubic rotations* and denoted by  $O$ . This is

the symmetry group for the zero total-momentum states. The octahedral group has five irreducible representations. In our study, we are interested in projecting onto the two-particle states with angular momentum  $l = 1$ . In order to understand in what sense — if at all — we can construct operators with certain angular momentum, we must determine how the angular momenta *mix* among the irreducible representations of the cubic group. To do this we first note that since the spherical harmonics act as a basis for the full rotation group, they will constitute a basis for any subset of the full rotation group. To determine how the angular momenta mix among the irreducible representations of the cubic rotations, one computes the characters associated with the  $l^{\text{th}}$  basis of spherical harmonics. The resultant characters can then be compared to the characters of the five irreducible representations to determine which combination (direct sum) build up the  $l^{\text{th}}$  representation. The results are displayed in table 2. The arguments for case 2 follow similarly. The relevant symmetry group is the *tetragonal group*. The tetragonal group consist of the subset of cubic rotations which leave the  $z$ -coordinate either invariant or reflected. The resolution of the  $2l + 1$  dimensional representations associated with the spherical harmonics into the irreducible representations of the tetragonal group is displayed in table 3. From tables 2 and 3, we can determine how the angular momentum mix. The results are shown in table 1 . To summarize, we have shown that the reduction of rotational symmetry has made it impossible to create a filter which leaves only states corresponding to a single angular momentum in the spectral decomposition of the correlation function. In general, the more the rotational symmetry is reduced the weaker the filter becomes. Consider the case of  $l = 0$ . If the Hamiltonian is invariant under the full rotation group, we can create a filter which selects only the states with  $l = 0$ . If the rotational symmetry is reduced to the cubic rotations then the best we can do is create a filter by projecting onto the  $A_2$ . This filter will then selects the states with angular momentum  $l = 0, 4, 6...$  (see table 1). Therefore there will be contamination from states with  $l \geq 4$ . If the rotational symmetry is *further* reduced to the tetragonal rotations, the best filter we can construct will have contamination from states with angular momentum  $l \geq 2$ .

Table 1: This table shows how the angular momentum mix among the irreducible representations of the octahedral and tetragonal groups

cubic rotations		tetragonal rotations	
irreducible representation	$l$	irreducible representation	$l$
$A_1$	0,4,6 ...	$A_1$	0,2,3...
$A_2$	3,6, ...	$A_2$	1,3,4...
$F_1$	1,3,4,5,6 ...	$B_1$	2,3,4...
$F_2$	2,3,4,5,6 ...	$B_2$	2,3,4...
$E$	2,4,5,6 ...	$E$	1,2,3,4...

Table 2: This table displays the resolution of the angular momentum into the irreducible representations of the octahedral group

Characters of the classes of $O$						Resolution into irreducible representations
1	E	$C_3$	$C_4^2$	$C_2$	$C_4$	
0	1	1	1	1	1	$A_1$
1	3	0	-1	-1	1	$F_1$
2	5	-1	1	1	-1	$E \oplus F_2$
3	7	1	-1	-1	-1	$A_2 \oplus F_1 \oplus F_2$
4	9	0	1	1	1	$A_1 \oplus E \oplus F_1 \oplus F_2$
5	11	-1	-1	-1	1	$E \oplus 2F_1 \oplus F_2$
6	13	1	1	1	-1	$A_1 \oplus A_2 \oplus E \oplus F_1 \oplus 2F_2$

Table 3: This table displays the resolution of the angular momentum into the irreducible representations of the tetragonal group

Characters of the classes of $D_4$						Resolution into irreducible representations
1	E	$C_4^2$	$C_4$	$C_2$	$C_2'$	
0	1	1	1	1	1	$A_1$
1	3	-1	1	-1	-1	$A_2 \oplus E$
2	5	1	-1	1	1	$A_1 \oplus B_1 \oplus B_2 \oplus E$
3	7	-1	-1	-1	-1	$A_2 \oplus B_1 \oplus B_2 \oplus 2E$
4	9	1	1	1	1	$2A_1 \oplus A_2 \oplus B_1 \oplus B_2 \oplus 2E$

It is often also desired to project onto a state of definite parity as is the case in this investigation. The relevant group contains two elements, the identity  $E$  and the parity transformation  $P$ . It has two irreducible representations. This group is abelian and hence all irreducible representations are one-dimensional. Using these facts and  $P^2 = E$ , it is a simple matter to construct the character table. The results are displayed in table 4. At this point we give an example of the formalism presented thus far. We consider the projection of a function  $f(x)$  onto the irreducible representation of the parity group (see table 4), i.e. we project onto the even and odd parts of  $f(x)$ . Applying the projection operator defined in Eq. 28 gives

$$f_{A_2}(x) = \frac{1}{2} \{ \chi^{A_2}(E) O_E f(x) + \chi^{A_2}(P) O_P f(x) \} \quad (38)$$

$$= \frac{1}{2} \{ f(x) - f(-x) \} \quad (39)$$

and

$$f_{A_1}(x) = \frac{1}{2} \{ \chi^{A_1}(E) O_E f(x) + \chi^{A_1}(P) O_P f(x) \} \quad (40)$$

$$= \frac{1}{2} \{ f(x) + f(-x) \} \quad (41)$$

Table 4: Character table for the parity group

E	P	irreducible representation
1	1	$A_1$ (positive)
1	-1	$A_2$ (negative)

As expected,  $f_{A_1}(x)$  and  $f_{A_2}(x)$  are even and odd respectively.

Lastly, we will be interested in projecting out the states with a certain momentum. The relevant group to study is the translation group. The translation group is a good symmetry since it preserves the condition of periodicity and is an exact symmetry even on a spatially *discretized* torus. The translational group is abelian and therefore all the irreducible representations are one-dimensional and may be chosen as unitary. To basis functions for the irreducible representations can be — and normally are — chosen to be

$$\psi_{\mathbf{p}}(\mathbf{r}) = \exp[i\mathbf{p} \cdot \mathbf{r}] \quad (42)$$

The action of the group on  $\psi_{\mathbf{p}}(\mathbf{r})$  is then

$$D(\mathbf{a})\psi_{\mathbf{p}}(\mathbf{r}) = \psi_{\mathbf{p}}(\mathbf{r} + \mathbf{a}) = \exp[i\mathbf{p} \cdot \mathbf{a}] \psi_{\mathbf{p}}(\mathbf{r}) \quad (43)$$

where each value of  $\mathbf{p}$  constitutes a *non-equivalent* irreducible representation.

In this study, we will perform calculations on a spatial lattice with periodic boundary conditions. We first consider the effect of discretization by considering an infinite spatial lattice. In this case, the translational group becomes an infinite discrete group. The irreducible representations of this group can no longer be classified uniquely by a momentum  $\mathbf{p}$ . The momenta associated with equivalent representations can be determined by finding all the representations which have identical characters. This leads to the condition

$$(\mathbf{p}_1 - \mathbf{p}_2) \cdot \mathbf{a} = 2\pi\mathbf{m} \quad (44)$$

where  $\mathbf{a}_i = a_i n_i \vec{\mathbf{e}}_i$ ,  $a_i$  is the distance between lattice points, and  $n_i \in \mathbb{Z}$ . One finds that the set of momentum with  $|p| \leq 2\pi/a$  is sufficient to label all the irreducible representations. The set of momenta defined in this way comprise the first *the first Brillouin zone*. As a result of this reduction in translational symmetry, functions defined on the lattice can no longer take on any value for the momentum. Instead one finds that the momenta are restricted to values

$$-\frac{\pi}{a} \leq p_i < \frac{\pi}{a} \quad (45)$$

The periodic boundary conditions quantize the momenta so that they take values

$$\mathbf{p}_{\mathbf{n}} = \frac{2\pi}{L} \mathbf{n} \quad \mathbf{n} \in \mathbb{Z}^3 \quad (46)$$

where  $L$  denotes the period, and for simplicity is taken to be the the same in all directions. The calculations in this investigation will be done with functions defined on a spatially discretized periodic box. As a result the momenta must satisfy both Eq. 45 and 46. The set of momenta obeying these two conditions is

$$\mathbf{p}_{\mathbf{n}} = \frac{2\pi}{L} \mathbf{n} \quad \mathbf{n} \in \Gamma \quad (47)$$

where

$$\Gamma = \{\mathbf{p}_n \in \mathbb{R}^3 \mid n_i = 0, 1, 2, \dots, N - 1\} \quad (48)$$

## 4.2 Variational Method

In section 2, we saw that the general technique for extracting physical quantities using lattice QCD is to fit the long time behavior of correlation functions. The correlation function  $C(t)$  is obtained stochastically, and as a result statistical errors on the values of  $C(t)$  lead to practical difficulties. In this section, we will present a method for calculating the low-lying energies when the values are nearly degenerate — a difficulty that plagues the low-lying two-particle spectrum for large boxes. One method used for the extraction of such a spectrum is referred to as the *variational method* and was proposed by M. Lüscher and U. Wolff [1].

To understand the the variational method, we start by considering the correlation function

$$C(t_2, t_1) = \langle 0|T \{O(t_2)^\dagger O(t_1)\} |0\rangle - \langle 0|O(t_2)^\dagger|0\rangle \langle 0|O(t_1)|0\rangle \quad (49)$$

The functional form follows from Eq. 9 and is given by

$$C(t) = \sum_{n=1}^{\infty} c_n^* c_n \exp(-W_n t) \quad (50)$$

where  $W_n = E_n - E_0$  with  $E_0$  representing the vacuum energy,  $t = t_2 - t_1$  and  $c_n = \langle 0|O|n\rangle$ . We argued that by choosing  $t$  properly, the correlation function is well approximated by a finite sum over the low-lying energies  $W_n$ . However, if the energies are not well separated the values of  $t$  will have to be large. This requires substantially more computational time since the lattice size in  $t$  has to increase; also the signal-to-noise ratio decreases. One possible avenue to overcome this is to construct a matrix of correlation functions using different interpolating operators which have the same quantum numbers. To this end we define the correlation matrix

$$C(t)_{ij} = \langle 0|T \{O_i(t_2)^\dagger O_j(t_1)\} |0\rangle - \langle 0|O_i(t_2)^\dagger|0\rangle \langle 0|O_j(t_1)|0\rangle \quad (51)$$

$$= \sum_{n=1}^{\infty} c_i^{*n} c_j^n \exp(-W_n t) \quad (52)$$

where  $i, j = 1, 2, \dots, r$  and the energies are ordered in increasing value. It was shown in [1] that the eigenvalues of  $C(t)$  are given by

$$\lim_{t \rightarrow \infty} \lambda_n(t) = c_n e^{-W_n t} \{1 + O(e^{-\Delta W_n t})\} \quad (53)$$

where  $c_n > 0$  and  $\Delta W_n$  is the minimum distance from the other spectral values  $n > r$ . As a result, there is a larger separation between the leading exponential and sub-leading exponentials. Each eigenvalue can then be fitted to a single exponential for an appropriately large value of  $t$ , and the  $r$  lowest energies can be extracted. A similar method was proposed which is expected to converge more rapidly with time. This method considers the eigenvalues of the generalized eigenvalue problem

$$C(t)\psi = \lambda(t, t_o)C(t_o)\psi \quad (54)$$

The eigenvalues of this equation are still given by Eq. 53 except the coefficients  $c_n$  and the coefficients of the sub-leading exponentials are different. In particular, one expects  $c_n \approx e^{t_0 W_n}$  while the higher order correction terms are suppressed [1].

To summarize, we need to measure the ground state for the moving frame and the first excited state for the CM frame. Due to the near degeneracies in the low-lying spectrum, we must construct a matrix of correlation functions. In the case of the ground state, the minimum dimensions of the matrix should be  $2 \times 2$ . If the first excited state is not well separated from the second then we will require at least a  $3 \times 3$  matrix of correlation functions.

### 4.3 Construction of interpolating fields

As discussed in subsection 4.2, in order to extract the first excited state it is necessary to construct a matrix of correlation functions with the same quantum numbers. Our goal is to extract the first two energies in the spectrum with a  $2 \times 2$  matrix. In this section, we will discuss the construction of two interpolating fields with the quantum numbers of the  $\rho$  meson using the tools developed in subsection 4.1.

We start by constructing interpolating fields with the same quantum numbers as the  $\rho$ -mesons. The  $\rho$ -mesons have quantum numbers  $(I)J^{PC} = (1)1^{--}$ . We consider the isospin representation  $|I, I_z\rangle$  which forms an isospin triplet. The simplest interpolating fields that one can write down with these quantum numbers are

$$\rho^-(x) = \bar{u}^a(x)\vec{\gamma}d^a(x) \quad \rho^+(x) = \bar{d}^a(x)\vec{\gamma}u^a(x) \quad \rho^0(x) = \frac{1}{2} \{ \bar{u}^a(x)\vec{\gamma}u^a(x) - \bar{d}^a(x)\vec{\gamma}d^a(x) \} \quad (55)$$

where  $\vec{\gamma}$  stands for either  $\gamma_1, \gamma_2$  or  $\gamma_3$ ,  $x$  is a four-dimensional position, and the repeated superscripts represent a trace over the color indices. In the isospin limit the masses of the ‘‘up’’ and ‘‘down’’ quarks are degenerate. We then project the fields onto a certain momentum. Restricting our attention to the neutral  $\rho$ -meson, one has

$$\rho^0(t, \mathbf{p} = 0) = \frac{1}{N^3} \sum_{\mathbf{x} \in \Gamma} \rho^0(\mathbf{x}, \mathbf{t}) \quad \text{and} \quad \rho^0(t, \mathbf{p}) = \frac{1}{N^3} \sum_{\mathbf{x} \in \Gamma} e^{i\mathbf{p} \cdot \mathbf{x}} \rho^0(\mathbf{x}, \mathbf{t}) \quad (56)$$

where

$$\Gamma = \{ \mathbf{x} \in \mathbb{R}^3 \mid x_i = an_i, n_i = 0, 1, 2, \dots, N-1 \}, \quad (57)$$

$a$  is the lattice spacing taken to be the same in all spatial directions, and  $N$  is the number of lattice points per direction. To create a second interpolating field, we consider two-pion states with zero total-momentum ( $\mathbf{P} = 0$ ). In the isospin representation, the pions form the isospin triplet

$$\pi^- = |1, -1\rangle \quad \pi^+ = |1, 1\rangle \quad \pi^0 = |1, 0\rangle \quad (58)$$

The simplest interpolating fields with these quantum numbers are

$$\pi^-(x) = \bar{u}^a(x)\gamma_5 d^a(x) \quad \pi^+(x) = \bar{d}^a(x)\gamma_5 u^a(x) \quad \pi^0(x) = \frac{1}{2} \{ \bar{u}^a(x)\gamma_5 u^a(x) - \bar{d}^a(x)\gamma_5 d^a(x) \} \quad (59)$$

Coupling the two pions together, one finds for  $I = 1$

$$|1, -1\rangle = \frac{1}{\sqrt{2}} \{ \pi^0 \pi^- - \pi^- \pi^0 \} \quad (60)$$

$$|1, 1\rangle = \frac{1}{\sqrt{2}} \{ \pi^+ \pi^0 - \pi^0 \pi^+ \} \quad (61)$$

$$|1, 0\rangle = \frac{1}{\sqrt{2}} \{ \pi^+ \pi^- - \pi^- \pi^+ \} \quad (62)$$

We again consider the isospin channel  $|1, 0\rangle$ . Projection onto zero total-momentum gives

$$\begin{aligned} \pi\pi(\mathbf{x}_1, \mathbf{x}_2, t) &= \frac{1}{\sqrt{2}N^3} \sum_{\mathbf{a} \in T} \pi^+(\mathbf{x}_1 - \mathbf{a}, t) \pi^-(\mathbf{x}_2 - \mathbf{a}, t) \\ &\quad - \frac{1}{\sqrt{2}N^3} \sum_{\mathbf{a} \in T} \pi^-(\mathbf{x}_1 - \mathbf{a}, t) \pi^+(\mathbf{x}_2 - \mathbf{a}, t) \end{aligned} \quad (63)$$

where  $T$  is an element of the translation group. Letting  $\mathbf{x} = \mathbf{x}_1 - \mathbf{a}$ ,  $\mathbf{r} = \mathbf{x}_2 - \mathbf{x}_1$ , and using the periodicity, Eq. 64 can be written as

$$\pi\pi(\mathbf{r}, t) = \frac{1}{\sqrt{2}N^3} \sum_{\mathbf{x} \in \Gamma} \{ \pi^+(\mathbf{x}, t) \pi^-(\mathbf{x} + \mathbf{r}, t) - \pi^-(\mathbf{x}, t) \pi^+(\mathbf{x} + \mathbf{r}, t) \} \quad (64)$$

The next task is to project out the component of  $\pi\pi(\mathbf{r}, t)$  with angular momentum  $J = 1$ . As discussed in subsection 4.1 this cannot be done exactly. Instead we project onto the  $F_1$  representation of the cubic group  $O$  which allows states with angular momentum  $J = 1, 3, 4, 5, 6, \dots$ . One has

$$\pi\pi(\mathbf{r}, t)_{F_1} = \frac{3}{24} \sum_{R \in O} \chi^{F_1}(R) \pi\pi(R^{-1}\mathbf{r}, t) \quad (65)$$

Lastly, since the  $\rho$ -mesons have odd parity we must project out the even part of  $\pi\pi(\mathbf{r}, t)_{F_1}$ . This gives

$$\pi\pi(\mathbf{r}, t)_{F_1^-} = \frac{1}{2} [\pi\pi(\mathbf{r}, t)_{F_1} - \pi\pi(-\mathbf{r}, t)_{F_1}] \quad (66)$$

$\pi\pi(\mathbf{r}, t)_{F_1^-}$  now represents an operator which will excite states with the quantum numbers of two pions and angular momentum  $l = 1, 3, 5, \dots$  in the CM with back to back momentum  $\mathbf{p}$ . At this point, we have almost succeeded in creating an operator with the correct quantum numbers. Due to the reduction of the rotational symmetry this is the best we can do. We have seen that the vacuum expectation value is a sum of decaying exponentials with respect to time which are weighted by the energies with the symmetries of the interpolating operators. The states with angular momentum  $J \geq 3$  correspond to larger energies and therefore the ground and first excited states can be taken to correspond to states with angular momentum  $J = 1$ . The construction of the interpolating fields required for asymmetric boxes follows identically except the projection onto the  $F_1$  irreducible representations of the octahedral group is replaced with a projection onto the  $A_2$  irreducible representation of the tetragonal group.

The last case to consider is the moving frame. In this case, the calculation is done on a cubic box with periodic boundary conditions where the total-momentum of the pions is non-zero. The energy in the lab  $W_L$  is then used to determine the energy in the CM frame. Taking the momentum



to be along one of the spatial axes reduces the symmetry in the CM to the tetragonal group. We then require an interpolating field in the lab frame which after a boost to the CM frame is a basis for either the  $A_2^-$  or  $E^-$  irreducible representation of the tetragonal group. We choose to project onto the  $A_2^-$  representation. The  $E^-$  representation would work just as well and could be used to create a third interpolating field. Here we will work backwards. We start by writing the interpolating field in lab frame and then show that after a boost the operator belongs to  $A_2^-$  irreducible representation. We consider the interpolating field corresponding to one pion with a momentum  $\mathbf{p}_1 = 2\pi/L\vec{e}_z$  and the other at rest. The total-momentum in this case is  $\mathbf{P} = 2\pi/L\vec{e}_z$ . The corresponding interpolating field is

$$\pi\pi(\mathbf{p}_1, t; 0, t) = \frac{1}{\sqrt{2}N^6} \sum_{\mathbf{x}_1, \mathbf{x}_2 \in \Gamma} \exp\{i\mathbf{p}_1 \cdot \mathbf{x}_1\} \{\pi^+(\mathbf{x}_1, t)\pi^-(\mathbf{x}_2, t) - \pi^-(\mathbf{x}_1, t)\pi^+(\mathbf{x}_2, t)\} \quad (67)$$

Performing the boost along the  $z$ -directions gives

$$\pi\pi(\mathbf{p}_1/2, t; -\mathbf{p}_1/2, t) = \frac{1}{\sqrt{2}} \{\pi^+(\mathbf{p}_1/2, t)\pi^-(\mathbf{p}_1/2, t) - \pi^-(\mathbf{p}_1/2, t)\pi^+(\mathbf{p}_1/2, t)\} \quad (68)$$

Applying the projection operator for the tetragonal and parity group, one finds that this operator is indeed a basis for the  $A_2^-$  irreducible representation. More succinctly,

$$P_{A_2^-}\pi\pi(\mathbf{p}_1/2, t; -\mathbf{p}_1/2, t) = \pi\pi(\mathbf{p}_1/2, t; -\mathbf{p}_1/2, t) \quad (69)$$

To see this, we note that  $\pi(\mathbf{p})$  transforms under rotation and parity according to

$$O_R\pi(\mathbf{p}) = \pi(R\mathbf{p}) \quad \text{and} \quad O_P\pi(\mathbf{p}) = -\pi(P\mathbf{p}) \quad (70)$$

Since  $\mathbf{p}_1$  is in the  $z$ -direction, under the tetragonal rotations it is left either invariant in which case  $\pi\pi(\mathbf{p}_1/2, t; -\mathbf{p}_1/2, t)$  is unchanged or it flips signs. In the latter case, one has

$$O_R\pi\pi(\mathbf{p}_1/2, t; -\mathbf{p}_1/2, t) = \frac{1}{\sqrt{2}} \{\pi^+(\mathbf{p}_1/2, t)\pi^-(\mathbf{p}_1/2, t) - \pi^-(\mathbf{p}_1/2, t)\pi^+(\mathbf{p}_1/2, t)\} \quad (71)$$

Using the fact that the interpolating fields  $\pi^+$  and  $\pi^-$  commute gives

$$O_R\pi\pi(\mathbf{p}_1/2, t; -\mathbf{p}_1/2, t) = -\frac{1}{\sqrt{2}} \{\pi^+(\mathbf{p}_1/2, t)\pi^-(\mathbf{p}_1/2, t) - \pi^-(\mathbf{p}_1/2, t)\pi^+(\mathbf{p}_1/2, t)\} \quad (72)$$

Performing the projection sum and noting that the characters for the rotations leaving  $z$  invariant are 1 and the characters for the rotations reflecting  $z$  are -1, one finds that Eq. 69 is valid. The case for parity follows similarly.

#### 4.4 Evaluation of the correlation matrix

In this section, we discuss the procedure for determining the correlation matrix. In general, one starts by writing the vacuum expectation value of the interpolating operators in terms of quark contractions  $\overline{\psi}^\dagger\psi$  where  $\psi$  is a quark field of a given flavor. The quark contractions are equal to the inverse fermionic matrix. Denoting the fermionic matrix by  $M$ , we have

$$\overline{\psi_i^{\dagger b}(y)\psi_j^a(x)} = M_{yib, xja}^{-1} \quad (73)$$

The fermionic matrix is constructed from the lattice gauge fields referred to as a *gauge configuration*. The evaluation of the correlation matrix for a given gauge configuration then amounts to the numerical computation of the inverse of the fermionic matrix — in fact this is where the largest computational resources are required.

For this investigation, we need to calculate the correlation matrix for an ensemble of gauge configurations. Using the operators discussed in section 4.3, the correlation matrix takes the form

$$G(t) = \begin{pmatrix} \langle \pi\pi^\dagger(t_2)\pi\pi(t_1) \rangle & \langle \pi\pi^\dagger(t_2)\rho(t_1) \rangle \\ \langle \rho^\dagger(t_2)\pi\pi(t_1) \rangle & \langle \rho^\dagger(t_2)\rho(t_1) \rangle \end{pmatrix} \quad (74)$$

where the representation label has been dropped,  $t = t_2 - t_1$ , and the  $\langle \cdot \rangle$  is to be understood as the vacuum expectation value. As discussed previously, the matrix elements of  $G(t)$  are constructed from interpolating fields which have certain quantum numbers. In particular, each of the four matrix elements is obtained by performing an appropriate sum over one of the four interpolating fields

$$\pi\pi^\dagger(\mathbf{x}_2, t_2)\pi\pi(\mathbf{x}_1, t_1), \quad \rho^\dagger(\mathbf{x}_2, t_2)\rho(\mathbf{x}_1, t_1), \quad \pi\pi(\mathbf{x}_2, t_2)\rho(\mathbf{x}_1, t_1), \quad \rho^\dagger(\mathbf{x}_2, t_2)\pi\pi(\mathbf{x}_1, t_1) \quad (75)$$

For example,

$$G(t, \mathbf{r})_{\pi\pi \rightarrow \pi\pi} = \frac{1}{2N^6} \sum_{\mathbf{x}, \mathbf{y} \in \Gamma} \langle \pi\pi^\dagger(\mathbf{y}, \mathbf{y} + \mathbf{r}, t_2)\pi\pi(\mathbf{x}, \mathbf{x} + \mathbf{r}, t_1) \rangle \quad (76)$$

The other matrix elements are displayed in table 5 for  $\mathbf{r} = \vec{\mathbf{e}}_i$ . It is therefore sufficient to compute the contractions of the four interpolating fields defined in Eq. 75. Once the contractions are known the matrix elements can be calculated by performing the appropriate sum. The contractions for the four interpolating fields are displayed graphically in Fig. 2.

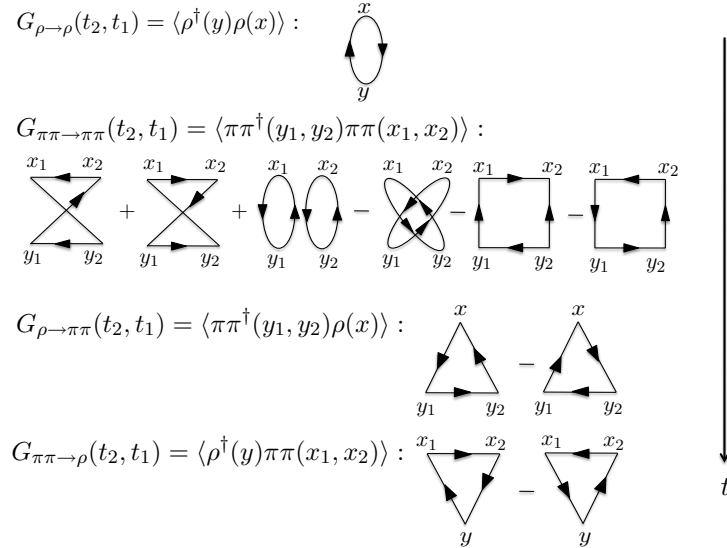


Figure 2: In this figure, the quark contractions for the four components required for the correlation matrix are shown.

To understand how to read these diagrams, we give a brief example. In particular, we will translate the the first triangular diagram in  $G_{\rho \rightarrow \pi\pi}(t_2, t_1)$ . Since, we are in the isospin limit the fermion matrices for the  $u$  and  $d$  quarks are identical and we use  $M^{-1}$  to denote either. There are three quark propagations between  $y_1, y_2$  and  $x$ ,  $x \rightarrow y_1, y_1 \rightarrow y_2$  and  $y_2 \rightarrow x$ . This translates into the product

$$M_{y_1, x}^{-1} M_{x, y_2}^{-1} M_{y_2, y_1}^{-1} \quad (77)$$

where the Dirac and color indices still need to be added in and the order of the position indices is important. Next we add the color indices. Since the trace is taken for all operators the color indices are at identical space-time points. This gives

$$M_{y_1 a, x b}^{-1} M_{x b, y_2 c}^{-1} M_{y_2 c, y_1 a}^{-1} \quad (78)$$

Next we add the Dirac indices all of which must be contracted. From section 4.3, we see that the  $\rho$  comes with a  $\vec{\gamma}$  and  $\pi$  with a  $\gamma_5$ . We also note that a left (right) Dirac index must be a left (right) index of the fermion matrix. Noting the position associated with the operators, we arrive finally at

$$(\gamma_5)_{ij} (\gamma_5)_{kl} (\vec{\gamma})_{mn} M_{y_1 i a, x n b}^{-1} M_{x b, y_2 l c}^{-1} M_{y_2 k c, y_1 j a}^{-1} \quad (79)$$

Having determined the contractions, we next need to determine the combinations of operators formed by the projection sums. To simplify the sums as much as possible, we take the position  $\mathbf{r}$  in  $\pi\pi(\mathbf{r}, t)$  to be along one of the axis ( $\mathbf{r} = \vec{\mathbf{e}}_i$ ). The results for  $G_{\pi\pi \rightarrow \rho}$  will be worked out explicitly. The others are displayed in Tab. 5. To do the projection, we generate all the cubic rotations in cartesian coordinates. This representation is equivalent to the  $F_1$  representation. Performing the sum leaves the two terms

$$\begin{aligned} & \frac{1}{2} \{ \pi\pi(\vec{\mathbf{e}}_i) - \pi\pi(-\vec{\mathbf{e}}_i) \} = \\ & \frac{1}{2\sqrt{2}N^3} \sum_{\mathbf{x} \in \Gamma} \{ \pi^+(\mathbf{x}, t) \pi^-(\mathbf{x} + \vec{\mathbf{e}}_i, t) - \pi^-(\mathbf{x}, t) \pi^+(\mathbf{x} + \vec{\mathbf{e}}_i, t) \} \\ & - \frac{1}{2\sqrt{2}N^3} \sum_{\mathbf{x} \in \Gamma} \{ \pi^+(\mathbf{x}, t) \pi^-(\mathbf{x} - \vec{\mathbf{e}}_i, t) - \pi^-(\mathbf{x}, t) \pi^+(\mathbf{x} - \vec{\mathbf{e}}_i, t) \} \end{aligned} \quad (80)$$

where

$$\Gamma = \{ \mathbf{x} \in \mathbb{R}^3 \mid x_i = a n_i, n_i = 0, 1, 2, \dots, N-1 \}, \quad (81)$$

$a$  is the lattice spacing taken to be the same in all spatial directions, and  $N$  is the number of lattice points per direction. If we use the commutation relations of  $\pi^+$  and  $\pi^-$  and rewrite the sum using the periodicity, we arrive at the rather simple result

$$P_{F_1^-} \pi\pi(\vec{\mathbf{e}}_i) = \frac{1}{\sqrt{2}N^3} \sum_{\mathbf{x} \in \Gamma} \{ \pi^+(\mathbf{x}, t) \pi^-(\mathbf{x} + \vec{\mathbf{e}}_i, t) - \pi^-(\mathbf{x}, t) \pi^+(\mathbf{x} + \vec{\mathbf{e}}_i, t) \}$$

The corresponding element of the correlation matrix is then given by

$$G(t)_{\pi\pi \rightarrow \rho} = \frac{1}{\sqrt{2}N^6} \sum_{\mathbf{x}, \mathbf{y} \in \Gamma} \langle \rho^{\dagger 0}(\mathbf{y}, t_2) \pi\pi(\mathbf{x}, \mathbf{x} + \vec{\mathbf{e}}_i, t_1) \rangle \quad (82)$$

where  $t = t_2 - t_1$ . The matrix elements can then be determined using the results of table 5 in combination with the quark contractions in Fig. 2.

Table 5: In this table, the appropriate projections sums are displayed.

center-of-mass frame	
$G(t)_{\pi\pi\rightarrow\pi\pi}$	$\frac{1}{2N^6} \sum_{\mathbf{x}, \mathbf{y} \in \Gamma} \langle \pi\pi^\dagger(\mathbf{y}, \mathbf{y} + \vec{\mathbf{e}}_i, t_2) \pi\pi(\mathbf{x}, \mathbf{x} + \vec{\mathbf{e}}_i, t_1) \rangle$
$G(t)_{\rho\rightarrow\pi\pi}$	$\frac{1}{\sqrt{2}N^6} \sum_{\mathbf{x}, \mathbf{y} \in \Gamma} \langle \pi\pi^\dagger(\mathbf{y}, \mathbf{y} + \vec{\mathbf{e}}_i, t_2) \rho^0(\mathbf{x}, t_1) \rangle$
$G(t)_{\pi\pi\rightarrow\rho}$	$\frac{1}{\sqrt{2}N^6} \sum_{\mathbf{x}, \mathbf{y} \in \Gamma} \langle \rho^{\dagger 0}(\mathbf{y}, t_2) \pi\pi(\mathbf{x}, \mathbf{x} + \vec{\mathbf{e}}_i, t_1) \rangle$
$G(t)_{\rho\rightarrow\rho}$	$\frac{1}{N^6} \sum_{\mathbf{x}, \mathbf{y} \in \Gamma} \langle \rho^{\dagger 0}(\mathbf{y}, t_2) \rho^0(\mathbf{x}, t_1) \rangle$
lab frame ( $\mathbf{P} \neq 0$ )	
$G(t)_{\pi\pi\rightarrow\pi\pi}$	$\frac{1}{2N^6} \sum_{\mathbf{y}_1, \mathbf{y}_2, \mathbf{x}_1, \mathbf{x}_2 \in \Gamma} \exp\{-i\mathbf{p} \cdot (\mathbf{y}_1 - \mathbf{x}_1)\} \langle \pi\pi^\dagger(\mathbf{y}_1, \mathbf{y}_2, t_2) \pi\pi(\mathbf{x}_1, \mathbf{x}_2, t_1) \rangle$
$G(t)_{\rho\rightarrow\pi\pi}$	$\frac{1}{\sqrt{2}N^6} \sum_{\mathbf{y}_1, \mathbf{y}_2, \mathbf{x} \in \Gamma} \exp\{-i\mathbf{p} \cdot (\mathbf{y}_1 - \mathbf{x})\} \langle \pi\pi^\dagger(\mathbf{y}_1, \mathbf{y}_2, t_2) \rho^0(\mathbf{x}, t_1) \rangle$
$G(t)_{\pi\pi\rightarrow\rho}$	$\frac{1}{\sqrt{2}N^6} \sum_{\mathbf{x}_1, \mathbf{x}_2, \mathbf{y} \in \Gamma} \exp\{-i\mathbf{p} \cdot (\mathbf{y} - \mathbf{x}_1)\} \langle \rho^{\dagger 0}(\mathbf{y}, t_2) \pi\pi(\mathbf{x}_1, \mathbf{x}_2, t_1) \rangle$
$G(t)_{\rho\rightarrow\rho}$	$\frac{1}{N^6} \sum_{\mathbf{x}, \mathbf{y} \in \Gamma} \exp\{-i\mathbf{p} \cdot (\mathbf{y} - \mathbf{x})\} \langle \rho^{\dagger 0}(\mathbf{y}, t_2) \rho^0(\mathbf{x}, t_1) \rangle$

## 5 Simulation Parameters

In this section, we discuss the practical feasibility of investigating the  $\rho$ -meson decay-width. As discussed previously, the energy regime where the  $\rho$ -meson decays for unphysical pion masses can be estimated by using values of  $(m_\pi, m_\rho)$  in the literature. We also argued that the most readily accessible energies are the ground and first excited states. It is also necessary to have box sizes with spatial extent large enough so that the finite volume effects are negligible as well as a sufficiently fine lattice spacing so that discretization errors are negligible. The finite volume effects decay exponentially as  $e^{-m_\pi L}$ . In practice, one requires  $m_\pi L \geq 3$ . Therefore the use of smaller pion masses requires larger boxes which in turn requires more computational resources. This is compounded by the fact that as the pion mass decreases the inversion of the fermionic matrix requires also requires substantially more computational resources. From experience, the lattice spacing  $a$  is chosen to be no greater than 0.1 fm. To determine the lattice parameters, we vary  $m_\pi$  and establish whether the  $\rho$ -meson decays in a regime which satisfies the latter mentioned conditions and which is feasible with current computational resources. We then determine what spatial lattice volume  $V$  is required with a lattice spacing of 0.1 fm. Once the volume is known the required computational resources can be estimated. The spatial lattice volume is defined as

$$V = N_x N_y N_z \quad (83)$$

where  $N_x = L_x/a_x$ ,  $N_y = L_y/a_y$ , and  $N_z = L_z/a_z$ . Once the lattice volume is determine, one can estimate the amount of computational resources required and decide whether it is feasible with current resources. We found  $m_\pi = 330$  MeV to be a suitable pion mass. In Fig. 3, we reproduce Fig. 1 in lattice units. The physical case is also shown for completeness. From the Fig. 3, we see that the volumes required for the CM and moving frames are  $V = 40^3$  and  $V = 20^3$  respectively.

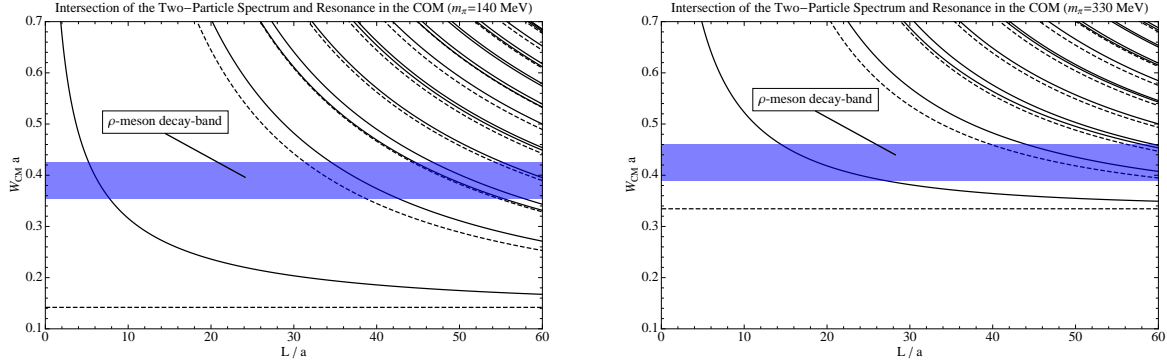


Figure 3: In this figure, the non-interacting two-particle spectrum is plotted in lattice units for  $m_\pi = 330$  MeV and  $m_\pi = 140$  MeV. The dashed lines correspond to the CM energies obtained when the lab frame and CM coincide. The solid lines represent the spectrum in the CM when the lab frame and CM are moving relative to each other with a momentum  $\mathbf{P} = \frac{2\pi}{L}\vec{e}_z$ . The blue bands represent the energy regime where the  $\rho$ -meson decays. For the non-physical pion mass the energy regime where for  $\rho$  resonance is determined by looking at previously determined values of  $(m_\pi, m_\rho)$  in the literature while the decay-width is taken to be the same as the physical one.

## 6 Conclusions

In conclusion, we propose to calculate the decay width of the  $\rho$ -meson as seen in the  $P$ -wave scattering channel of the two-pion system with isospin  $I = 1$  via lattice QCD. Our motivation is two fold: to improve on previous attempts and hence demonstrate the ability of QCD to predict the experimental value and to build the framework for future studies in this area.

## References

- [1] M. Lüscher and U. Wolff, Nucl. Phys. **B339**, 222 (1990).
- [2] M. Lüscher, Nucl. Phys. **B354**, 531 (1991).
- [3] S. R. Beane, K. Orginos, and M. J. Savage, IJMPE **17**, 1157 (2008).
- [4] N. Ishii, S. Aoki, and T. Hatsuda, Phys. Rev. Lett. **99**, 02201 (2007).
- [5] S. Aoki *et al.*, Phys. Rev. **B76**, 094506 (2008).
- [6] X. Feng, K. Jansen, and D. B. Renner, arXiv.org:0910.4871 [hep-lat], 2009.
- [7] G. Rios, A. Nicola, C. Hanhart, and J. Pelaez, arXiv:0905.3489v1 [hep-lat], 2008.
- [8] H. Rother, *Lattice Gauge Theories: An Introduction*, 3 ed. (World Scientific Publishing Company, 2005).
- [9] J. Smit, *introduction to Quantum Fields on a Lattice* (Cambridge University Press, 2002).
- [10] I. montvay and G. Münster, *Quantum Fields on a Lattice* (Cambridge University Press, 1997).
- [11] Feynman and Hibbs, *Quantum Mechanics and Path Integrals* (McGraw-Hill Companies, 1965).
- [12] K. Rummukainen and S. Gottlieb, Nucl. Phys. **B450**, 397 (1995).
- [13] M. Göckeler *et al.*, arXiv.org:0810.5337v1 [hep-lat], 2009.
- [14] M. Hammermesh, *Group Theory and Its Application to Physical Systems* (Dover Publications, 1989).